Geometric Eddington factor for radiative transfer problems

Julien Cartier, Alexandre Munnier

Geometric Eddington Factor for radiative transfer problems

J. Cartier[*], *A. Munnier*[†]

Abstract. In this paper, a geometric closure method for radiative transfer equations has been developed and investigated using particular geometric configurations. Then, we propose a new formulation of the Eddington factor (and the related flux limiter) adapted to radiative transfer calculations, whereas classical Eddington's approximation cannot be applied. Moreover, a numerical scheme and numerical results for the new flux limiter are presented in two dimensions configurations.

Key words: Radiative transfer, diffusion approximation, Eddington factor, flux limiter.

1. Introduction

Inertial Confinment Fusion (ICF) is a way to achieve thermonuclear fusion in a laboratory: it consists in imploding a small target of hydrogen so that high temperature and high density lead to the burn of a large fraction of fuel. The more efficient way to obtain a quasi-isotropic implosion is to use the radiation flux created by conversion of Laser energy into X-ray in the wall of an Hohlraum (see figure 1).

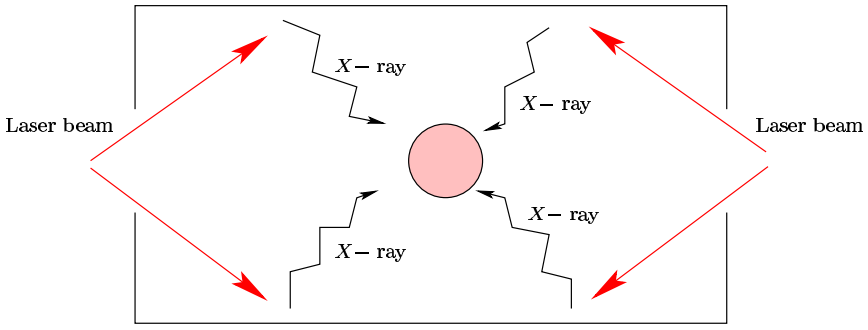

Figure 1: Hohlraum cavity

Radiative transfer equations describe the transport of X-ray energy in the Hohlraum, neglecting hydrodynamic motion it writes as:

$$\frac{1}{c}\partial_t I + \vec{\Omega}\cdot\vec{\nabla}_x I + \sigma_\nu I = \frac{c}{4\pi}\sigma_\nu S(\nu,T), \tag{1.1}$$

where $I(x,\vec{\Omega},\nu,t)$ is the radiative intensity ($\vec{\Omega}$ takes its values in the unit sphere $\mathcal{S}^2$ and the frequency ν is strictly positive), c is the speed of light and σ_ν is the opacity. The intensity $I(x,\vec{\Omega},\nu,t)$ is related to the distribution function of a photon gas that is of a population of particles travelling in straight lines at the speed of light c. The source function $S(\nu,T)$ is the so-called Planck function which depends on the temperature T so that equation (1.1) is coupled to an energy balance equation:

$$\partial_t E_i(T) + \int_{\mathcal{S}^2} d\vec{\Omega} \int_{\nu>0} d\nu\, \sigma_\nu (I - \frac{c}{4\pi}S(\nu,T)) = 0, \tag{1.2}$$

where E_i is the internal energy.
The usual method for solving system (1.1)(1.2) consists in using an implicit Monte-Carlo method (see [3] for example). However, Monte-Carlo oscillations of the solution alter the required symmetry of the radiation field and can cause an incorrect calculation of the implosion. On the other hand, deterministic methods (see [2]) are very costly and cannot be used for parametric studies. This is why it is useful to obtain approximate models for radiative transfer problems. The goal of this paper is to present a new closure for (1.1)(1.2) that can be used in the ICF context. In order to simplify the analysis, we will restrict ourselves to a simplified version of (1.1)(1.2): first, we consider a stationary problem (i.e. we solve the system on one single time step). Secondly, we assume that the source function is given so that frequency variable can be removed and (1.1) becomes:

$$\vec{\Omega}\cdot\vec{\nabla}_x I + \sigma I = \frac{c}{4\pi}\sigma S. \tag{1.3}$$

At last, we impose boundary conditions that account for albedo of the gold wall. For each x on the boundary and each incoming direction $\vec{\Omega}$ we impose:

$$I(x,\vec{\Omega}) = \frac{1-\omega}{\pi}\int_{\vec{\Omega}.\vec{n}_b>0} I(x,\vec{\Omega}')\vec{\Omega}'.\vec{n}_b\, d\vec{\Omega}', \tag{1.4}$$

where $\vec{n}_b$ is the unit normal outward vector at the boundary point x. For the sake of simplicity, we only consider a model geometry (see figure 2).

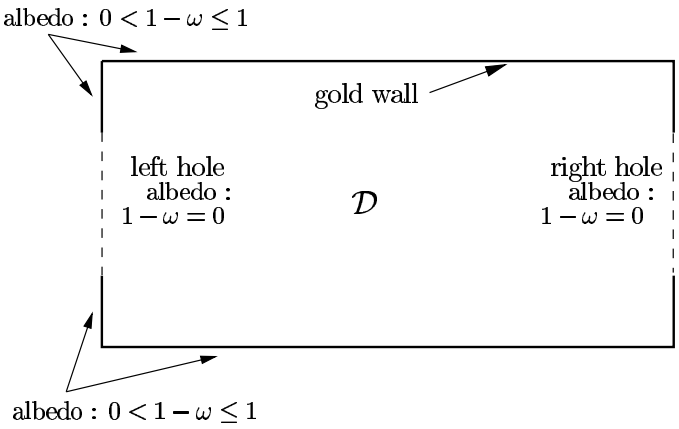

Figure 2: Model geometry

When opacity is large, it is well known (see [4]) that diffusion approximation can be applied to system (1.3)(1.4). In this limit, radiative energy E_r is solution of a diffusion equation:

$$-\mathrm{div}\left(\frac{1}{3\sigma}\nabla E_r\right) + \sigma E_r = \sigma S, \quad E_r := \frac{1}{c}\int_{\mathcal{S}^2} I(x,\vec{\Omega})\, d\vec{\Omega}. \tag{1.5}$$

In an Hohlraum this assumption does not hold: the cavity is usually filled with a low density gas and the photon mean free path in the gas (σ^{-1}) is large compared to typical dimension of the device. So limit (1.5) which corresponds to the small mean free path limit is no longer valid.
However, it is always possible at least formally, to define a corrected diffusion limit

$$-\mathrm{div}\left(\frac{\lambda}{\sigma}\nabla E_r\right) + \sigma E_r = \sigma S, \quad E_r := \frac{1}{c}\int_{\mathcal{S}^2} I(x,\vec{\Omega})\, d\vec{\Omega}, \tag{1.6}$$

where λ is related to the Eddington factor γ so that equation (1.6) provides a correct approximation of the solution. This is our purpose to discuss this method and to propose a calculation of the Eddington factor adapted to our problem.
The outline of the paper is the following: in next section, we describe the calculation of γ in the Hohlraum. Then, we analyse its properties with respect to the general theory of Eddington factors of [5]. In section 4, we give some details on the numerical scheme for the non-linear diffusion equation. At last, we present numerical results showing the interest of our approach and we compare them with usual flux-limited diffusion theory.

2. Calculation of Eddington factor

Let us consider the radiative transfer equation:

$$\begin{cases} \vec{\Omega}\cdot\vec{\nabla}I(x,\vec{\Omega}) + \sigma\, I(x,\vec{\Omega}) = \dfrac{c}{4\pi}\,\sigma\, S(x), & (x,\vec{\Omega}) \in \mathcal{D}\times\mathcal{S} \\ I(x,\vec{\Omega}) = \dfrac{1-\omega}{\pi}\displaystyle\int_{\vec{\Omega}'\cdot\vec{n}>0} I(x,\vec{\Omega}')\,\vec{\Omega}'\cdot\vec{n}\; d\vec{\Omega}', & x\in\partial\mathcal{D},\ \vec{\Omega}\cdot\vec{n}<0. \end{cases} \tag{2.7}$$

Here, $1-\omega$ denotes the albedo of the wall and is defined as the ratio between incoming and outcoming radiative fluxes at the boundary. The geometrical configuration that we consider in the sequel is described in figure 3.

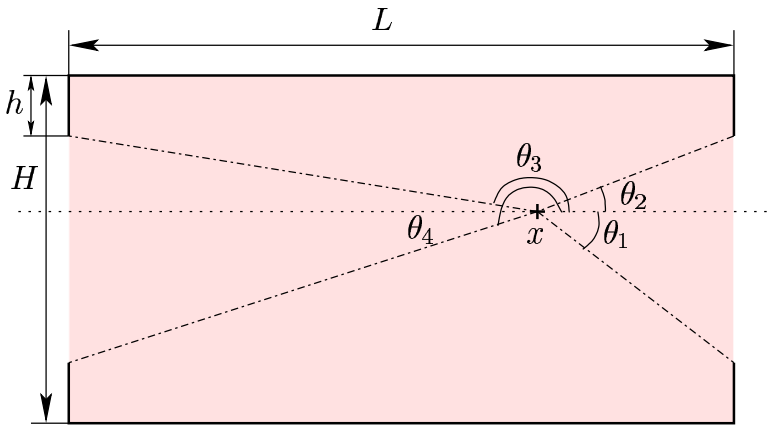

Figure 3: Geometric configuration

We also introduce:

$$E(x) := \frac{1}{c}\int_{4\pi} I(x,\vec{\Omega})\, d\vec{\Omega}, \quad \text{(radiative energy density)}, \tag{2.8}$$

$$\vec{F}(x) := \int_{4\pi} I(x,\vec{\Omega})\,\vec{\Omega}\, d\vec{\Omega}, \quad \text{(radiative flux)}, \tag{2.9}$$

$$[P(x)] := \frac{1}{c}\int_{4\pi} I(x,\vec{\Omega})\,\vec{\Omega}\otimes\vec{\Omega}\, d\vec{\Omega}, \quad \text{(radiative pressure tensor)},$$

and the Eddington tensor $[\gamma]$ which is defined by the relation :

$$[\gamma] := \frac{[P]}{E}.$$

We apply the so-called "moment method" which consists in integrating the first equation of (2.7) over the solid angles $\vec{\Omega}$. We get :

$$\frac{1}{c}\vec{\nabla}\cdot\vec{F} + \sigma\, E = \sigma\, S \quad \text{in } \mathcal{D}. \tag{2.10}$$

Multiplying the first line of (2.7) by $\vec{\Omega}$ and integrating over directions $\vec{\Omega}$, we obtain:

$$\operatorname{div}[P] + \frac{\sigma}{c}\vec{F} = 0 \quad \text{in } \mathcal{D}, \tag{2.11}$$

that is:

$$-\operatorname{div}(\frac{1}{\sigma}\operatorname{div}([\gamma]E)) + \sigma E = \sigma S \quad \text{in } \mathcal{D}. \tag{2.12}$$

When σ is large, diffusion approximation applies (see [4]) and the Eddington factor becomes constant:

$$[\gamma] = \frac{1}{3}[Id]. \tag{2.13}$$

In this case, radiative transfer equation can be replaced by a diffusion equation (the so-called Rosseland approximation).
In our situation the diffusion approximation (1.5) is not valid but it is always possible to replace formally the transport equation by a diffusion equation provided that the Eddington Tensor is correctly defined: we refer here to the review paper [5] which explains how a flux-limited diffusion equation can in some sense approximate a transport equation. We want to apply this method in our case, but using specific informations about the geometry we can improve the calculation of the Eddington factor (and hence of the flux-limiter) and obtain better results.

We have to consider now the following model with a flux-limiter λ:

$$\begin{cases} -\operatorname{div}(\frac{\lambda}{\sigma}\vec{\nabla}E) + \sigma E = \sigma S & \text{in } \mathcal{D}, \\ \omega E + 2(2-\omega)\frac{\lambda}{\sigma}\vec{\nabla}E \cdot \vec{n}_b = 0 & \text{on } \partial\mathcal{D}, \end{cases} \tag{2.14}$$

where λ is related to the Eddington factor $[\gamma]$ (see section 3.2). Our aim is to determine an algebraic expression of λ in such a way that the solution of the approximated problem (2.14) is close (in a formal sense) to the solution of the transport problem. We impose that λ (and the related Eddington factor) only depends on:

- a gradient length $\dfrac{|\vec{\nabla}E|}{E}$.
- geometrical data.

We briefly described how the boundary condition for the diffusion equation has been derived:
We first introduce the quantities $F := \vec{F}.\vec{n}_b$ on $\partial\mathcal{D}$ and $F^+ := \int_{\vec{\Omega}'.\vec{n}_b>0} I(x,\vec{\Omega}')\vec{\Omega}' \cdot \vec{n}_b \, d\vec{\Omega}'$ and $F^- := \int_{\vec{\Omega}'.\vec{n}_b<0} I(x,\vec{\Omega}')\vec{\Omega}'.\vec{n}_b \, d\vec{\Omega}'$ such that $F = F^+ - F^-$. According to the definition of the albedo, $F^- = (1-\omega)F^+$ and hence, $F^+ - F^- = \omega F^+ = F$.

On the other hand

$$F = \vec{F} \cdot \vec{n}_b = -\frac{\lambda c}{\sigma} \vec{\nabla} E \cdot \vec{n}_b. \tag{2.15}$$

Furthermore, we assume the following quasilinear P1 approximation:

$$I(x, \vec{\Omega}) = \frac{cE}{4\pi} + \frac{3}{4\pi} \vec{\Omega} \cdot \vec{F}. \tag{2.16}$$

Hence we get:

$$\omega F^+ = \omega \int_{\vec{\Omega}' \cdot \vec{n}_b > 0} \left(\frac{cE}{4\pi} + \frac{3}{4\pi} \vec{\Omega}' \cdot \vec{F} \right) \vec{\Omega}' . \vec{n}_b \, d\vec{\Omega}', \tag{2.17}$$

and

$$\omega F^+ = 2\pi\omega \int_0^1 \left(\frac{cE}{4\pi} - \frac{3\mu\lambda c}{4\pi\sigma} \vec{\nabla} E \cdot \vec{n}_b \right) \mu d\mu = \omega \frac{cE}{4} - \frac{\omega}{2} \frac{c\lambda}{\sigma} \vec{\nabla} E \cdot \vec{n}_b. \tag{2.18}$$

Summarizing (2.15) and (2.18), we obtain the boundary condition for the energy E:

$$\omega \, E + 2\,(2-\omega) \frac{\lambda}{\sigma} \vec{\nabla} E \cdot \vec{n}_b = 0. \tag{2.19}$$

Remark 2.1. The quantity $\dfrac{2\,(2-\omega)}{\omega} \dfrac{\lambda}{\sigma}$ is called the extrapolation length.

3. Computation of the Eddington Tensor $[\gamma]$

In order to compute $[\gamma]$, we apply a method inspired by the one developped in [6] for spherical problems: we assume that the radiative intensity at a given point x in $\mathcal{D}$ is piecewise constant with respect to the solid angle variable $\vec{\Omega}$.

3.1. The two intensities model

We first introduce some notations: let us define $S_T(x)$ as the part of $\mathcal{S}^2$ containing all the solid angles that link point x to the holes and $S_T{}^c(x) = \mathcal{S}^2 \setminus S_T(x)$. We make the following modelling assumption:

$$I(x, \vec{\Omega}) = \begin{cases} I_1(x) & \text{when } \vec{\Omega} \in S_T(x) \\ \\ I_2(x) & \text{when } \vec{\Omega} \in S_T{}^c(x). \end{cases} \tag{3.20}$$

This modelling can be justified by considering the numerical solution of the transport equation obtained with the classical DSN method: figure 4 presents the in-

tensity as a function of $\vec{\Omega}$ at a given point x in $\mathcal{D}$ close to the right hole. We clearly see that it is piecewise constant over S_T and S_T^c.

The intensity $I_1(x)$ is the mean radiative intensity resulting from the emission of the holes (and the medium) and $I_2(x)$ is the intensity resulting from the emission of the wall (and the medium). We also define:

$$\alpha_1 := \int_{S_T} d\vec{\Omega} \quad \text{and} \quad \alpha_2 := \int_{S_{T^c}} d\vec{\Omega}, \tag{3.21a}$$

the vectors :

$$\vec{v}_1 := \int_{S_T} \vec{\Omega}\, d\vec{\Omega} \quad \text{and} \quad \vec{v}_2 := \int_{S_{T^c}} \vec{\Omega}\, d\vec{\Omega}, \tag{3.21b}$$

and finally the tensors :

$$[m_1] := \int_{S_T} \vec{\Omega} \otimes \vec{\Omega}\, d\vec{\Omega} \quad \text{and} \quad [m_2] := \int_{S_{T^c}} \vec{\Omega} \otimes \vec{\Omega}\, d\vec{\Omega}. \tag{3.21c}$$

The analytical expressions of all these data will be given in the Appendix A. Using our assumption we obtain the following system :

$$\begin{cases} E = \dfrac{1}{c} I_1 \displaystyle\int_{S_T} d\vec{\Omega} + \dfrac{1}{c} I_2 \int_{S_{T^c}} d\vec{\Omega} \\ \vec{F} = I_1 \displaystyle\int_{S_T} \vec{\Omega}\, d\vec{\Omega} + I_2 \int_{S_{T^c}} \vec{\Omega}\, d\vec{\Omega} \\ [\gamma]\, E = \dfrac{1}{c} I_1 \displaystyle\int_{S_T} \vec{\Omega} \otimes \vec{\Omega}\, d\vec{\Omega} + \dfrac{1}{c} I_2 \int_{S_{T^c}} \vec{\Omega} \otimes \vec{\Omega}\, d\vec{\Omega}, \end{cases} \tag{3.22}$$

where the unknowns are I_1, I_2 and $[\gamma]$. Nevertheless, it is not possible to solve this system directly because $[\gamma]$ is a tensor. In order to solve the system, we will project the second and third equations along an appropriate direction.

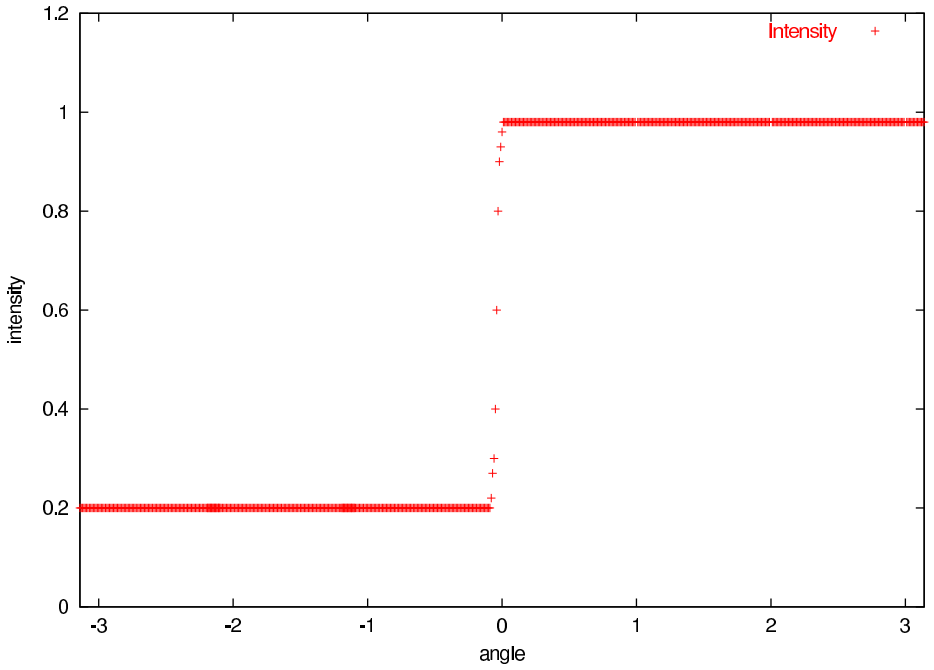

Figure 4: Intensity with respect to angle, close to the right hole of the domain $\mathcal{D}$ (results obtained on a uniform 100×100 grid in space and S_{64} quadrature for velocities).

3.1.1. Solution of the system It is easily seen that the following relations hold:

$$\alpha_1 + \alpha_2 = 4\pi, \tag{3.23a}$$
$$\vec{v}_1 + \vec{v}_2 = 0, \tag{3.23b}$$

and

$$[m_1] + [m_2] = \frac{4}{3}\pi\,[Id]. \tag{3.23c}$$

Applying (3.23) to (3.22), the system under considerations reads:

$$\begin{cases} 1 = \alpha_1 \bar{u}_1 + 4\pi u_2 \\ \vec{f} = \vec{v}_1 \bar{u}_1 \\ [\gamma] = [m_1]\bar{u}_1 + \dfrac{4\pi}{3}[Id]u_2, \end{cases} \tag{3.24}$$

where

$$\vec{f} := \frac{\vec{F}}{cE}. \tag{3.25}$$

The new unknowns are:

$$\bar{u}_1 := \frac{1}{cE}(I_1 - I_2),\ u_2 := \frac{1}{cE} I_2 \ \text{ and } \ [\gamma].$$

Observe that f have to satisfy, as required in the flux-limited diffusion theory:

$$|\vec{f}| \leq 1. \tag{3.26}$$

Moreover, $\vec{f}$ and $[\gamma]$ (the first and second moment of a nonnegative unit intensity $\frac{I}{cE}$) must satisfy the following constraints :

$$\mathrm{tr}([\gamma]) = 1, \tag{3.27}$$

$$[\gamma] - \vec{f} \otimes \vec{f} \geq 0. \tag{3.28}$$

Multiplying by $\frac{1}{3}[Id]$ the first equation of the system (3.24) and substracting to the third equation we get:

$$\begin{cases} 1 = \alpha_1 \bar{u}_1 + 4\pi u_2 \\ \vec{f} = \vec{v}_1 \bar{u}_1 \\ [\gamma] = \frac{1}{3}[Id] + \left([m_1] - \frac{\alpha_1}{3}[Id]\right) \bar{u}_1. \end{cases} \tag{3.29}$$

3.1.2. Computation of a scalar Eddington factor γ According to [5], we are interested in finding a scalar Eddington factor γ defined by:

$$\gamma \vec{n} = [\gamma]\, \vec{n}. \tag{3.30}$$

where $\vec{n}$ is the unit vector $\vec{f}/|\vec{f}|$. This leads to the following relation (see [5]):

$$[\gamma] = \frac{1-\gamma}{2}[Id] + \frac{3\gamma - 1}{2} \vec{n} \otimes \vec{n}. \tag{3.31}$$

This model can be seen as a generalization of the classical Eddington approximation (2.13). In order to determine γ, we shall use the tensor $[\gamma]$ introduced in the previous subsection.

First of all, remark that $\vec{v}_1$ is an eigenvector of the matrix $[m_1]$ and denote m_1 the associated eigenvalue. Hence, we have:

$$[m_1]\frac{\vec{v}_1}{|\vec{v}_1|} = m_1 \frac{\vec{v}_1}{|\vec{v}_1|}. \tag{3.32}$$

The third equation of (3.29) shows that $\vec{v}_1$ is also an eigenvector of $[\gamma]$. Using (3.30) we obtain:

$$\gamma = \frac{1}{3} + m_1\,\bar{u}_1 - \frac{\alpha_1}{3}\,\bar{u}_1. \tag{3.33}$$

Then, we express $\bar{u}_1$ in terms of $\vec{f}$. The second equation of (3.29) shows that $\vec{v}_1$ has the same direction as $\vec{n}$ ($\vec{n} = -\frac{\vec{v}_1}{|\vec{v}_1|}$) and we get:

$$\bar{u}_1 = \frac{|\vec{f}|}{|\vec{v}_1|}.$$

Finally, we obtain:

$$\gamma = \frac{1}{3} + \frac{m_1 - \frac{\alpha_1}{3}}{|\vec{v}_1|}\frac{\left|\vec{F}\right|}{cE}. \tag{3.34}$$

We shall rewrite this expression as:

$$\gamma(f) = \frac{1}{3} - h_1 f, \tag{3.35}$$

where h_1 is defined by:

$$h_1 = \frac{\frac{\alpha_1}{3} - m_1}{|\vec{v}_1|} = \frac{\frac{1}{3}\int_{S_T} d\vec{\Omega} - \int_{S_T}(\vec{\Omega}\cdot\vec{n})^2\, d\vec{\Omega}}{|\int_{S_T}\vec{\Omega}\cdot\vec{n}\, d\vec{\Omega}|}, \tag{3.36}$$

and

$$f = \frac{\left|\vec{F}\right|}{cE}.$$

3.2. Computation of a flux limiter λ

In this section, we relate the Eddington factor γ to a flux-limiter λ. Let us consider again the moment system:

$$\vec{\nabla}\cdot(\vec{f}E) + \sigma\,(E - S) = 0 \tag{3.37}$$

$$\vec{\nabla}\cdot([\gamma]E) + \sigma\vec{f}E = 0. \tag{3.38}$$

Multiplying the equation (3.37) by $\vec{f}$ and substracting to equation (3.38), one obtains:

$$\vec{\nabla}\cdot[([\gamma] - \vec{f}\otimes\vec{f})E] + \sigma\vec{f}S = 0. \tag{3.39}$$

From now on, we assume that the spatial variations of $[\gamma]$ and $\vec{f}$ are small, and we deduce, according to [5], an algebraic relation between $[\gamma]$, $\vec{f}$, E and $\vec{\nabla}E$:

$$\left([\gamma] - \vec{f}\otimes\vec{f}\right)\vec{R} = \vec{f}, \tag{3.40}$$

where $\vec{R}$ is the dimensionless gradient defined by:

$$\vec{R} = -\frac{\vec{\nabla} E}{\sigma S}. \tag{3.41}$$

So $R := |\vec{R}|$ and f are related by the relation:

$$R = \frac{f}{\gamma(f) - f^2}. \tag{3.42}$$

This allows us to define the flux limiter λ as

$$f = \lambda(R)R \text{ or } \lambda(R) = \gamma(f) - f^2, \tag{3.43}$$

what yields the flux:

$$\vec{F} = -\frac{c\,\lambda(R)\vec{\nabla} E}{\sigma}. \tag{3.44}$$

We compute the flux limiter $\lambda(R)$ related to the Eddington factor $\gamma(f)$. We have:

$$\lambda(R) = \frac{1}{3} - h_1 \lambda(R) R - \lambda^2(R) R^2, \tag{3.45}$$

what yields:

$$\lambda(R) = \frac{2}{3\left(h_1 R - 1\right)^2 + \sqrt{9(1 - h_1 R)^2 + 12R^2}}. \tag{3.46}$$

4. Properties of γ and λ

This section is devoted to the behaviour of the scalar γ (and λ) with respect to σ and f.

In [5], Levermore gives four conditions that γ and λ must satisfy:

(C1) $\lambda(R) + \lambda(R)^2 R^2 \leq 1$.

(C2) $\gamma(0) = \frac{1}{3}$ and $\lambda(0) = \frac{1}{3}$.

(C3) $\lambda(R) + \lambda(R)^2 R^2$ is an increasing function of R.

(C4) $\gamma(f) - f^2$ is a decreasing function of f.

The conditions (C1), (C2) and (C4) are satisfied, but our flux limiter violates the condition (C3). In order to satisfy (C3), the Eddington factor must be increasing as a function of f and it is not the case here because h_1 is always positive, hence $\lambda(R) + \lambda(R)^2 R^2$ is decreasing as a function of R.

Influence of geometrical parameter h_1 We can see that, when h_1 is equal to zero our geometric limiter is equal to the first part of the Minerbo limiter related to the Eddington factor $\gamma(f) = \frac{1}{3}$.

Behaviour of λ for diffusive and void cases For diffusive cases, i.e. $\sigma >> 1$, the Eddington's approximation is valid and we can take $\lambda = \frac{1}{3}$. For our flux limiter, we get: $\lim_{\sigma \to +\infty} \lambda = \frac{1}{3}$, and for the void case: $\lim_{\sigma \to 0} \lambda = 0$.

Influence of gradient A main property of flux limiter is to decrease when the norm of the radiative energy gradient increase, thus we have: $\lim_{R \to 0} \lambda = \frac{1}{3}$, $\lim_{R \to +\infty} \lambda = 0$. When $f = 0$ there is no preferred direction, the intensity is isotropic and the Eddington approximation is valid : $\gamma(0) = \frac{1}{3}$ and $\lambda(0) = \frac{1}{3}$. Let us now compare in figure 5 our geometric flux limiter with other classical flux limiters for a fixed value of h_1 ($h_1 = 1$).

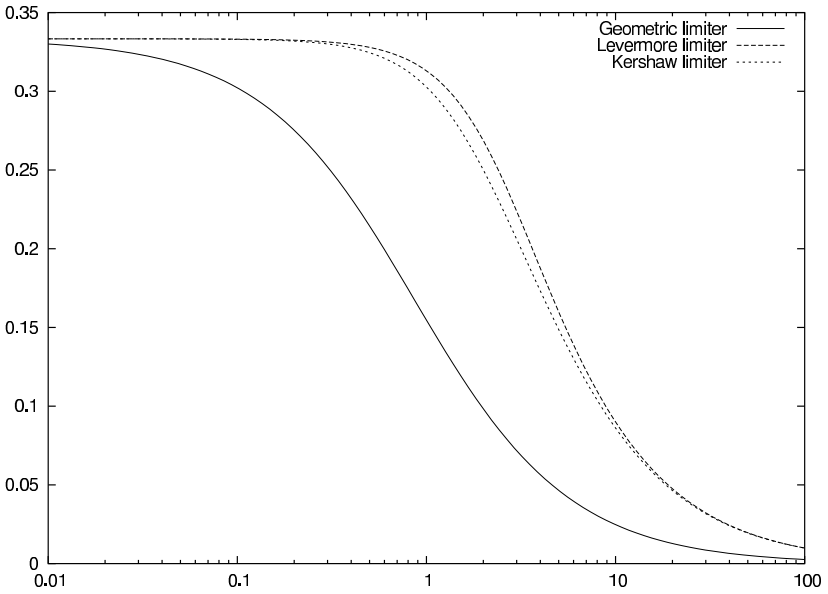

Figure 5: Behaviour of flux limiters when R increases

5. Numerical scheme

In order to solve the photon transport equation, we use the standard S_N method with the spatial diamond-differencing scheme. This is the reference transport method for a two-dimensional Cartesian fine mesh.

To solve the diffusion equation with a fixed flux limiter, we use a two-dimensional finite differences scheme coupled to a Jacobi algorithm. We also use a mixed-hybrid finite elements method (see [8]) in order to obtain more accuracy and to reduce the CPU time which becomes prohibitive when σ is small

Let us remark that no general result claiming the well-posedness of the nonlinear diffusion problem is available because of nonlinear dependence of the diffusion coefficient as a function of the gradient of the solution. Nevertheless, the flux limiter is bounded and positive and we observe convergence of the following fixed-point iterative method:

Step 1: Initialization : solve the diffusion equation with $\lambda(R) = \frac{1}{3}$ (Eddington's approximation):

$$\begin{cases} -\mathrm{div}\,(\frac{1}{3\sigma}\,\nabla E^0) + \sigma\, E^0 = \sigma\, S & \text{in } \mathcal{D}, \\ \omega\, E^0 + 2\,(2-\omega)\dfrac{1}{3\sigma}\vec{\nabla} E^0 \cdot \vec{n}_b = 0 & \text{on } \partial\mathcal{D}. \end{cases} \tag{5.47}$$

Step 2: We compute $R^0 = -\frac{|\vec{\nabla} E^0|}{S}$.

Step 3: For all $k \geq 0$, we compute a solution E^k of the diffusion problem with λ given by the expression of flux limiter, function of R^{k-1}:

$$\begin{cases} -\mathrm{div}\,(\frac{\lambda}{\sigma}\,(R^{k-1})\nabla E^k) + \sigma\, E^k = \sigma\, S & \text{in } \mathcal{D}, \\ \omega\, E^k + 2\,(2-\omega)\dfrac{\lambda(R^{k-1})}{\sigma}\vec{\nabla} E^k \cdot \vec{n}_b = 0 & \text{on } \partial\mathcal{D}. \end{cases} \tag{5.48}$$

Step 4: Then we compute $R^k = -\frac{|\vec{\nabla} E^k|}{S}$ and we loop to step 3 while $||E^k - E^{k-1}||_1$ becomes larger than a small arbitrary parameter.

6. Numerical Results

We first consider the case of two plane plates with reflecting conditions on the plane plates, entering flux equal to zero on the holes and a source equal to 1 (S=1). We compare in the figures 6, 7 and 8 a reference transport solution, a solution obtained by Eddington's approximation, a solution obtained with our model and a solution obtained with other flux limiters: Wilson's limiter [5], Chapman-Enskog's limiter [5] and Kershaw's limiter [5] for different values of σ. Let us give here the expressions of these flux limiters:

Wilson's limiter : $\lambda(R) = \frac{1}{3+R}$ and the related $\gamma(f) = \frac{1-f+3f^2}{3}$,

Chapman-Enskog's limiter : $\lambda(R) = \frac{1}{R}\left(\coth R - \frac{1}{R}\right)$ and the related $\gamma = \coth R\left(\coth R - \frac{1}{R}\right)$ with $f = \coth R - \frac{1}{R}$,

Kershaw's limiter : $\lambda(R) = \frac{2}{3+\sqrt{9+4R^2}}$ and the related $\gamma(f) = \frac{1+2f^2}{3}$.

The influence of these flux limiters will be compared to our geometrical model.

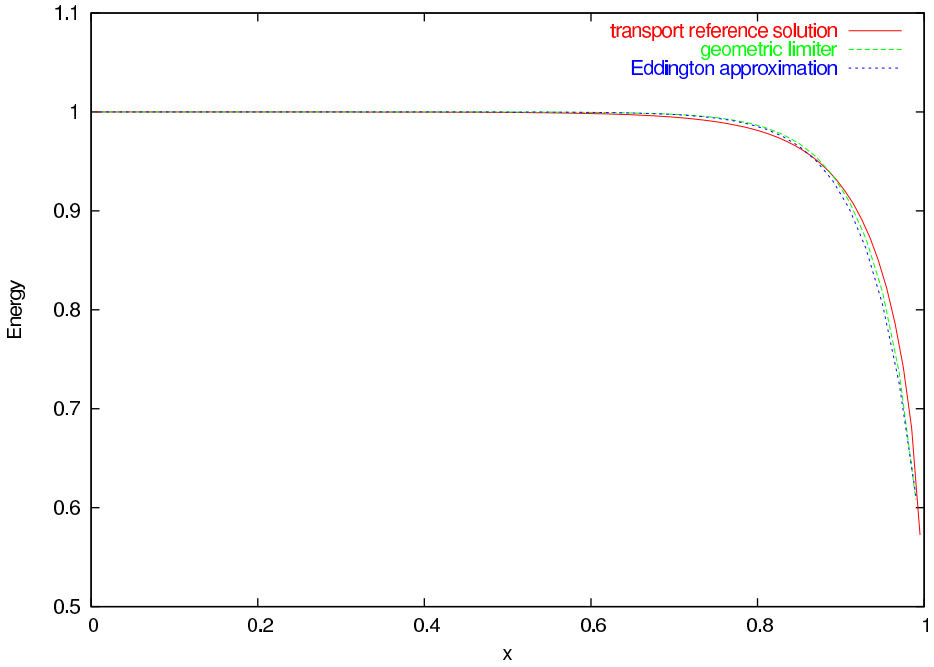

Figure 6: Section of energy for plane plates configuration in case of $\sigma = 10$

These numerical results are computed in two dimensions (on a 50×50 grid) but we just give a one-dimensional profile section of the energy in the figure and only in a quarter of domain $\mathcal{D}$ because of symmetry reasons. According to the notations of the figure 3, these numerical results was computed with the following parameters: $L = 2$, $H = 1$, $h = 0$ and the albedo of the wall $\omega = 0$.

One observes that the energy density are, in all cases considered, better approximated by the geometric method than by the diffusion's Eddington approximation (P1) or by the diffusion equation with classical flux limiters. It is particularly true for the region close to the hole where our geometric model seems clearly to be the most competitive method.

Figure 6 presents the profile of the energy in a case where σ is large. That means an isotropic case and it is why every model gives the same results. In figure 7, we show a case where opacity is smaller than the previous one. It seems that geometrical model is better than the others. When the opacity σ is close to zero,

the geometrical model always seems to be more efficient than the others but the flux-limiters results are too far away from the transport solution (as we can see in figure 8) because of the limits of validity of the model.

Indeed, we can compute, using the transport program, the effective ideal flux limiter given by the following relation:

$$\vec{F} = -\frac{c\lambda(R)\vec{\nabla}E}{\sigma}. \tag{6.49}$$

This flux limiter is the better one can expect with our model and it does not provide better results than the geometrical flux limiter.

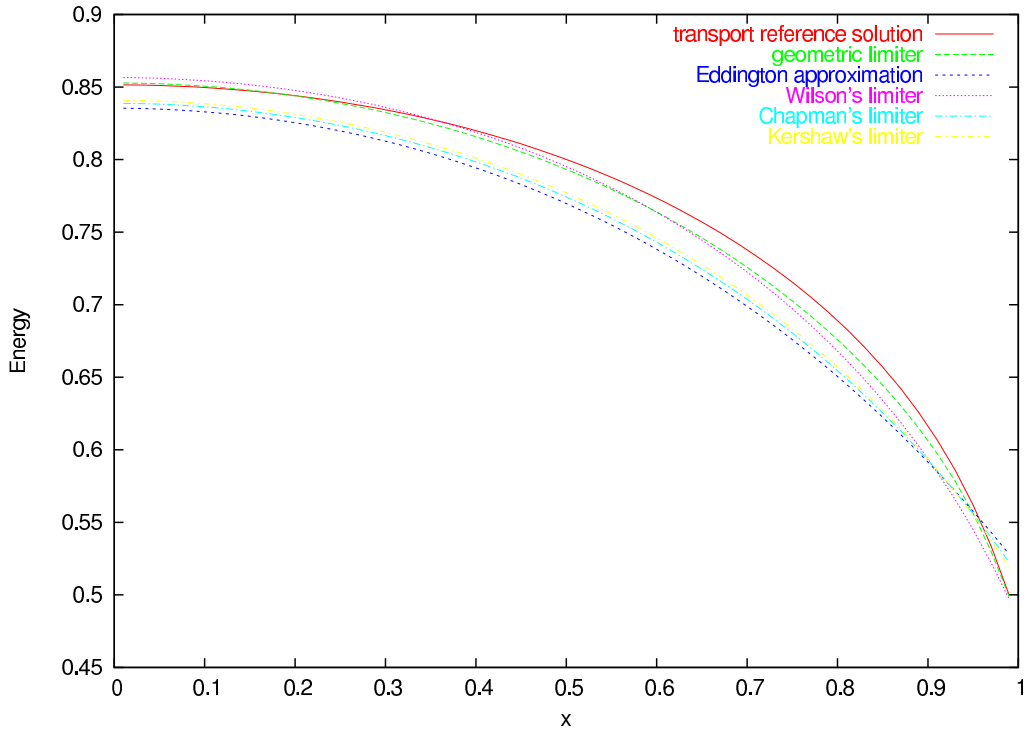

Figure 7: Section of energy for plane plates configuration in case of $\sigma = 1$

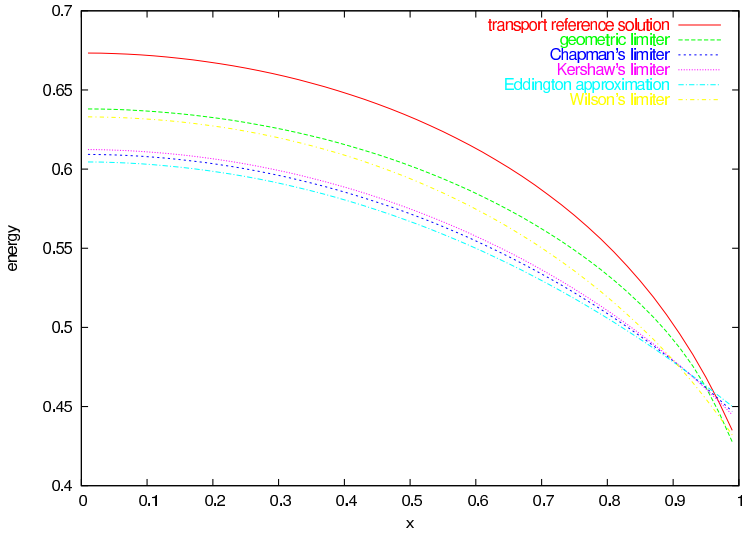

Figure 8: Section of energy for plane plates configuration in case of $\sigma = 0.5$

Let us now compare the results obtained with the "transport flux limiter" and the other ones in the figure 9:

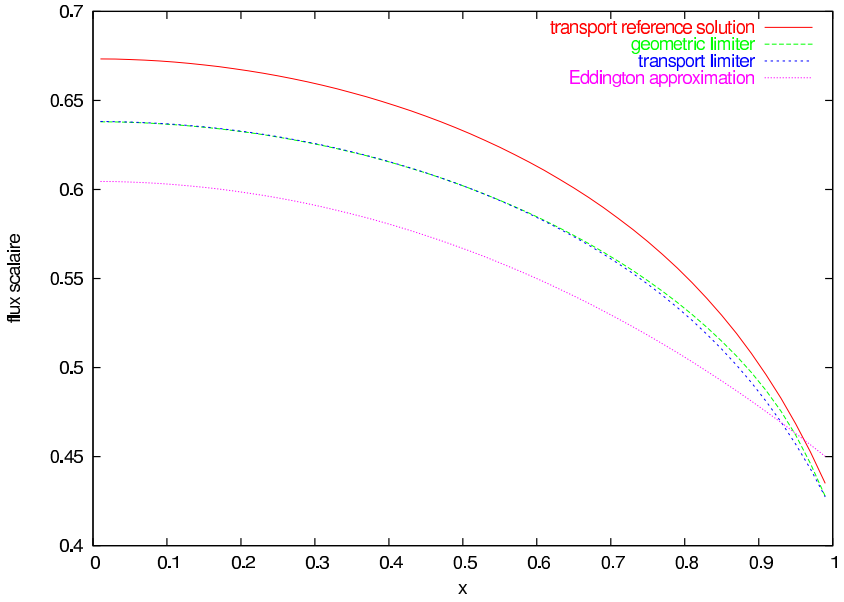

Figure 9: Section of energy for plane plates configuration in case of $\sigma = 0.5$

We can see that, even with the "transport flux limiter" the results are not close to the reference transport solution and our geometric limiter seems as good as the "transport flux limiter". When σ is close to zero, the diffusion model seems being not valid. Indeed, the "transport flux limiter" being obtained directly from the transport equation, it is optimal for our model.

We can also compare the profiles of the flux limiters as shown in figure 10:

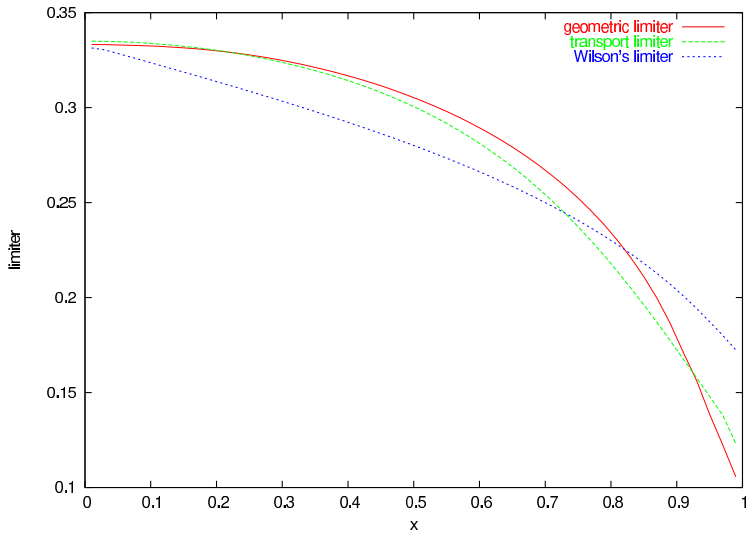

Figure 10: Profiles of flux limiters in case of $\sigma = 0.5$

Relative errors

We presents here a table containing the relative errors $\frac{||E_{dif} - E_{tra}||_1}{||E_{tra}||_1}$ between the transport reference solution and the solutions of our diffusion model for different flux limiters and some values of σ in the case of two plane plates.

	Geometric limiter	Wilson's limiter	Kershaw's limiter	Eddington's approx. (P1)
$\sigma = 10$	$2,63.10^{-3}$	$2,75.10^{-3}$	$3,02.10^{-3}$	$3,27.10^{-3}$
$\sigma = 1$	$7,94.10^{-3}$	$1,19.10^{-2}$	$2,66.10^{-2}$	$3,45.10^{-2}$
$\sigma = 0,5$	$4,42.10^{-2}$	$5,77.10^{-2}$	$8,22.10^{-2}$	$9,30.10^{-2}$

7. Conclusion

In this paper, we have proposed a new formulation of the Eddington factor (and the underlaying flux limiter) adapted to radiative transfer calculations in a cavity. The main point was that classical flux-limited diffusion theory did not apply because photon mean free path and gradient length of the solution are large in front of the size of the cavity so that geometric effects are dominant. Hence, the Eddington factor includes geometric features of the domain.
Although our modelling of the Eddington factor is correct, the corresponding results on the diffusion equation are not totally satisfactoring: our understanding is that the treatment of the boundary condition should be questionned. Future work will consist in applying this factor to realistic configurations (i.e. radiation hydrodynamic flows in an ICF cavity). In this case it may be necessary to improve the model in order to account for a more detailed description of the cavity (presence of the target, distinction between left and right laser entry holes,...).

Acknowledgements

This proceeding could not have been written without J.F. Clouet and G. Samba from CEA-DAM. The authors gratefully thank S. Cordier and B. Dubroca for their contributions to the present work.

A. Analytical expression of the data

The angles θ_i, $i = 1, 2, 3, 4$ are defined as shown in figure 3. We may then compute, according to the definitions (3.21), the following expressions:

$$\alpha_1 = 2\,(\theta_2 - \theta_1) + 2\,(\theta_4 - \theta_3) \tag{1.50}$$

$$\alpha_2 = 2\pi - \alpha_1. \tag{1.51}$$

We compute as well:

$$\vec{v}_1 = \int_{\theta_1}^{\theta_2}\int_{-1}^{1} \begin{pmatrix} -\sqrt{1-z^2}\cos\theta \\ -\sqrt{1-z^2}\sin\theta \end{pmatrix} dz\,d\theta + \int_{\theta_3}^{\theta_4}\int_{-1}^{1} \begin{pmatrix} -\sqrt{1-z^2}\cos\theta \\ -\sqrt{1-z^2}\sin\theta \end{pmatrix} dz\,d\theta.$$

Applying the change of variables $z = \sin t$, $dz = \cos t\,dt$, we get:

$$\begin{aligned} \int_{-1}^{1} \sqrt{1-z^2}\,dz &= \int_{-\pi/2}^{\pi/2} (\cos t)^2\,dt \\ &= \left[\frac{t}{2} + \frac{\cos 2t}{2}\right]_{-\pi/2}^{\pi/2} = \frac{\pi}{2}, \end{aligned}$$

and therefore, we obtain

$$\vec{v}_1 = -\frac{\pi}{2}\int_{\theta_1}^{\theta_2}\begin{pmatrix}\cos\theta\\ \sin\theta\end{pmatrix}d\theta - \frac{\pi}{2}\int_{\theta_3}^{\theta_4}\begin{pmatrix}\cos\theta\\ \sin\theta\end{pmatrix}d\theta, \tag{1.52}$$

that is:

$$\vec{v}_1 = \pi\sin\left(\frac{\theta_2-\theta_1}{2}\right)\begin{pmatrix}\cos\left(\frac{\theta_2+\theta_1}{2}\right)\\ \sin\left(\frac{\theta_2+\theta_1}{2}\right)\end{pmatrix} + \pi\sin\left(\frac{\theta_4-\theta_3}{2}\right)\begin{pmatrix}\cos\left(\frac{\theta_4+\theta_3}{2}\right)\\ \sin\left(\frac{\theta_4+\theta_3}{2}\right)\end{pmatrix}. \tag{1.53}$$

Then, we compute the expressions of $[m_1]$. The definition of $[m_1]$ is:

$$[m_1] = \int_{\theta_1}^{\theta_2}\int_{-1}^{1}[M(\theta,z)]\,dz\,d\theta + \int_{\theta_3}^{\theta_4}\int_{-1}^{1}[M(\theta,z)]\,dz\,d\theta,$$

where

$$[M(\theta,z)] = (1-z^2)\begin{pmatrix}(\cos\theta)^2 & \cos\theta\sin\theta\\ \cos\theta\sin\theta & (\sin\theta)^2\end{pmatrix}.$$

It is a simple matter to obtain $\displaystyle\int_{-1}^{1}(1-z^2)\,dz = \frac{4}{3}$ and

$$\int_{\theta_1}^{\theta_2}(\cos\theta)^2\,d\theta = \int_{\theta_1}^{\theta_2}\left[\frac{1}{2}+\frac{\cos 2\theta}{2}\right]_{\theta_1}^{\theta_2} = \frac{\theta_2-\theta_1}{2}+\left[\frac{\sin 2\theta}{4}\right]_{\theta_1}^{\theta_2}$$

and

$$\int_{\theta_1}^{\theta_2}(\sin\theta)^2\,d\theta = \frac{\theta_2-\theta_1}{2}-\left[\frac{\sin 2\theta}{4}\right]_{\theta_1}^{\theta_2}.$$

We also have:

$$\int_{\theta_1}^{\theta_2}\sin\theta\cos\theta\,d\theta = \left[\frac{1}{2}(\sin\theta)^2\right]_{\theta_1}^{\theta_2} = \frac{(\sin\theta_2)^2-(\sin\theta_1)^2}{2}.$$

Finally, we get:

$$[m_1] = \frac{4}{3}\begin{bmatrix}\frac{\theta_2-\theta_1}{2}+\frac{\sin 2\theta_2-\sin 2\theta_1}{4} & \frac{(\sin\theta_2)^2-(\sin\theta_1)^2}{2}\\ \frac{(\sin\theta_2)^2-(\sin\theta_1)^2}{2} & \frac{\theta_2-\theta_1}{2}-\frac{\sin 2\theta_2-\sin 2\theta_1}{4}\end{bmatrix} + \frac{4}{3}\begin{bmatrix}\frac{\theta_4-\theta_3}{2}+\frac{\sin 2\theta_4-\sin 2\theta_3}{4} & \frac{(\sin\theta_4)^2-(\sin\theta_3)^2}{2}\\ \frac{(\sin\theta_4)^2-(\sin\theta_3)^2}{2} & \frac{\theta_4-\theta_3}{2}-\frac{\sin 2\theta_4-\sin 2\theta_3}{4}\end{bmatrix}. \tag{1.54}$$

The expressions above simplify, using the trigonometric relations:

$$\begin{aligned}\sin 2\theta_2 - \sin 2\theta_1 &= 2\sin(\theta_2-\theta_1)\cos(\theta_1+\theta_1)\\ &= 4\sin\left(\frac{\theta_2-\theta_1}{2}\right)\cos\left(\frac{\theta_2-\theta_1}{2}\right)\cos(\theta_1+\theta_2),\end{aligned}$$

and

$$\begin{aligned}(\sin\theta_2)^2-(\sin\theta_1)^2 &= (\sin\theta_2-\sin\theta_1)(\sin\theta_2+\sin\theta_1)\\ &= 4\sin\left(\frac{\theta_2-\theta_1}{2}\right)\cos\left(\frac{\theta_1+\theta_2}{2}\right)\sin\left(\frac{\theta_2+\theta_1}{2}\right)\cos\left(\frac{\theta_2-\theta_1}{2}\right)\\ &= 2\sin\left(\frac{\theta_2-\theta_1}{2}\right)\cos\left(\frac{\theta_2-\theta_1}{2}\right)\sin(\theta_1+\theta_2).\end{aligned}$$

Hence, we obtain:

$$\begin{aligned}[\bar{m}_1] =&\\ &\frac{4}{3}\sin\left(\frac{\theta_2-\theta_1}{2}\right)\cos\left(\frac{\theta_2-\theta_1}{2}\right)\begin{bmatrix}\cos(\theta_1+\theta_2) & \sin(\theta_1+\theta_2)\\ \sin(\theta_1+\theta_2) & -\cos(\theta_1+\theta_2)\end{bmatrix}\\ &+\frac{4}{3}\sin\left(\frac{\theta_4-\theta_3}{2}\right)\cos\left(\frac{\theta_4-\theta_3}{2}\right)\begin{bmatrix}\cos(\theta_4+\theta_3) & \sin(\theta_4+\theta_3)\\ \sin(\theta_4+\theta_3) & -\cos(\theta_4+\theta_3)\end{bmatrix}.\end{aligned} \quad (1.55)$$

Combining expressions (1.52) and (1.55) of $\vec{v}_1$ and $[\bar{m}_1]$ with relation (3.22) from previous section, we obtain explicitly:

$$[\gamma] = [\gamma](\vec{R},\theta_1,\theta_2,\theta_3,\theta_4).$$

We can also compute the angles θ_i, $i=1,2,3,4$ with respect to the position (x,y) of the point, setting the origin $(0,0)$ at the center of the domain:

$$\begin{aligned}\theta_1(x,y) &= \arctan\left(\frac{-y-H/2+h}{L/2-x}\right)\\ \theta_2(x,y) &= \arctan\left(\frac{H/2-y-h}{L/2-x}\right)\\ \theta_3(x,y) &= \pi-\arctan\left(\frac{-y-H/2+h}{L/2+x}\right)\\ \theta_4(x,y) &= \pi-\arctan\left(\frac{H/2-y-h}{L/2+x}\right).\end{aligned}$$

B. Numerical results figures in two dimension

Cases between two plane plates ($h = 0$ and $\omega = 0$):

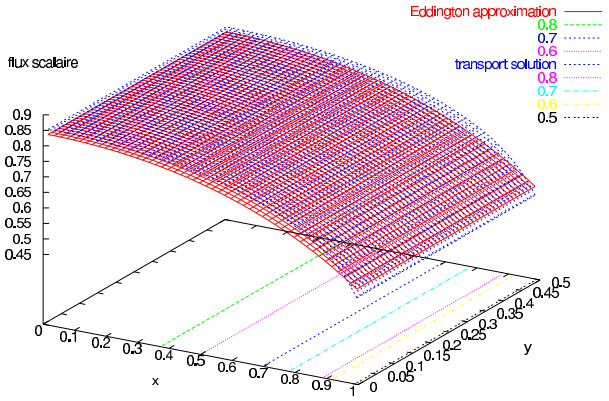

Figure 11: transport versus Eddington's approximation

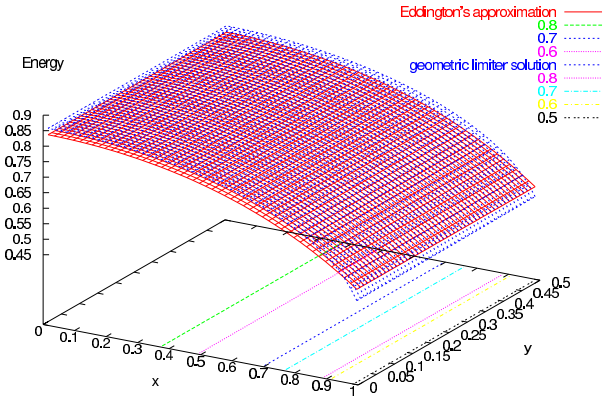

Figure 12: geometric limiter versus Eddington's approximation

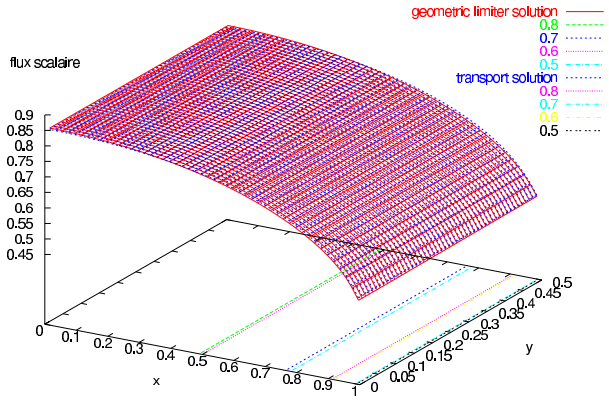

Figure 13: transport versus geometric limiter

Cases with edges ($h = 0.2$ and $\omega = 0.5$):

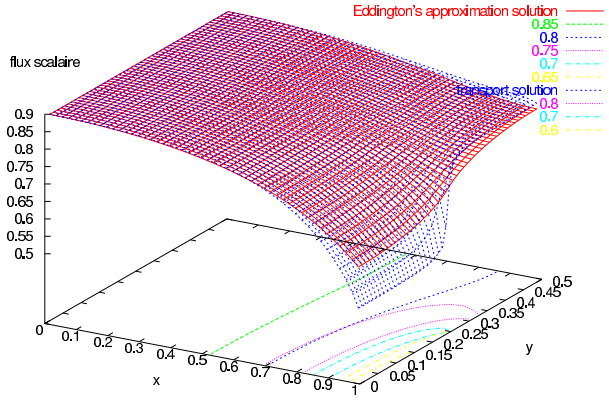

Figure 14: transport versus Eddington's approximation

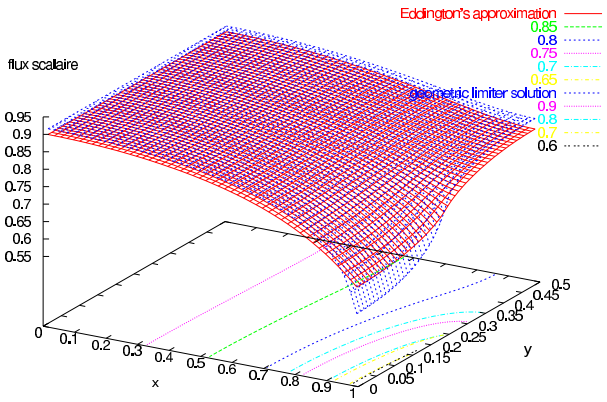

Figure 15: geometric limiter versus Eddington's approximation

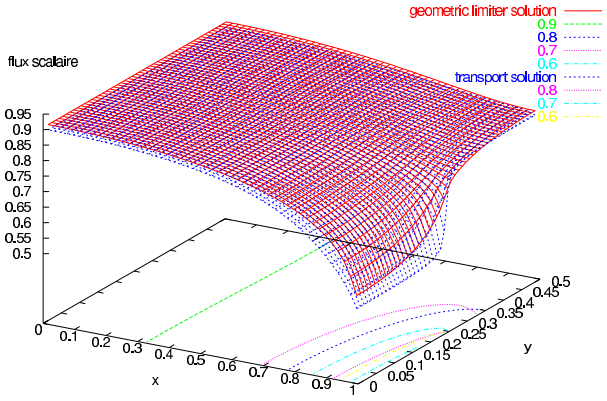

Figure 16: transport versus geometric limiter

References

[1] C.G.Pomraning, *The Equation of Radiation Hydrodynamics* , Pergamon Press, (1973).

[2] R.E.Alcouffe, B.A.Clark and E.W.Larsen, *The diffusion synthetic acceleration of transport iterations*, Multiple Time Scales, (J.Brackbill and B.Cohen ed.), Academic Press, New-York (1985).

[3] J.A.Fleck and J.D.Cummings, *An implict scheme for calculating time and frequency dependent non linear radiation transport*, J.Comp.Phys, 8 (1971).

[4] E.W.Larsen,V.C.Badham and G.C.Pomraning, *Asymptotic analysis of radiative transfer problems*, J.Quant.Spec.Radia.Transfer, 29 (1983).

[5] D.Levermore, *Relating Eddington factors to flux limiters* , J.Quant.Spec.Radia.Transfer, 26 (1984).

[6] M.Rampp and H.-Th.Janka, *Variable Eddington factor method for core-collapse supernova simulations* , A&A (2003)

[7] G.N.Minerbo, J.Quant.Spec.Radia.Transfer, 20 (1978).

[8] F.Brezzi and M.Fortin, *Mixed and hybrid finite element methods* , Springer-Verlag, New York (1991).